



LAWRENCE  
LIVERMORE  
NATIONAL  
LABORATORY

# Effect of Iron and Silica Nanoparticles' Size on in vitro Human Skin Binding and Penetration

E. Jung, X. Hui, H. Zhu, A. Zhang, W. Wang, B.  
Buchholz, H. Maibach

August 27, 2018

Toxicology Research and Application

## **Disclaimer**

---

This document was prepared as an account of work sponsored by an agency of the United States government. Neither the United States government nor Lawrence Livermore National Security, LLC, nor any of their employees makes any warranty, expressed or implied, or assumes any legal liability or responsibility for the accuracy, completeness, or usefulness of any information, apparatus, product, or process disclosed, or represents that its use would not infringe privately owned rights. Reference herein to any specific commercial product, process, or service by trade name, trademark, manufacturer, or otherwise does not necessarily constitute or imply its endorsement, recommendation, or favoring by the United States government or Lawrence Livermore National Security, LLC. The views and opinions of authors expressed herein do not necessarily state or reflect those of the United States government or Lawrence Livermore National Security, LLC, and shall not be used for advertising or product endorsement purposes.

Effect of iron and silica nanoparticles' size on in vitro human skin binding and penetration

Jung, Eui<sup>1</sup>; Hui, Xiaoying<sup>1\*</sup>; Zhu, Hanjiang<sup>1</sup>; Zhang, Alissa<sup>1</sup>; Wang, Wei<sup>2</sup>; Buchholz, Bruce<sup>3</sup>;  
Maibach, Howard<sup>1</sup>

\*Correspondence: [xiaoying.hui@ucsf.edu](mailto:xiaoying.hui@ucsf.edu)

<sup>1</sup>University of California San Francisco, School of Medicine, Dermatology, 90 Medical Center Way,  
Room 110, Box 0989, San Francisco, CA 94143

<sup>2</sup>Environmental Sciences Division, Oak Ridge National Laboratory, Oak Ridge, TN 37831, USA.  
(Current address: Aramco Research Center-Boston, Aramco Services Company, Cambridge, MA 02139,  
USA)

<sup>3</sup>Lawrence Livermore National Laboratory, Center for Accelerator Mass Spectrometry, 7000 East Avenue,  
Livermore, CA 94550

This work was performed in part under the auspices of the US Department of Energy by Lawrence  
Livermore National Laboratory under contract DE-AC52-07NA27344. Reviewed and released as LLNL-  
JRNL-757207.

## Introduction

The use of nanoparticles (NPs) has recently increased dramatically in diverse areas including industry, agriculture, medicine, and cosmetics<sup>1, 2, 3, 4, 5</sup>. Thus, their potential hazardous effects on human health are a matter of increasing interest and concern. The European Commission on Public Health<sup>6</sup> cautioned that NPs might have the ability to “stick” to molecular surfaces and cross cell membranes into a living system. NPs may interact with living systems, depending on the dimensions of both NPs and biomolecules such as proteins, if they are of similar size<sup>7</sup>. In a living system, if NPs dissolve easily they can spread through the entire body and exert chemical effects<sup>8</sup>. If NPs are not soluble, they may accumulate in biological systems and persist<sup>9</sup>.

Skin has a surface area of approximately 1.8 m<sup>2</sup> that acts as the primary physical barrier between our body and exogenous environmental factors<sup>10, 11</sup>. Dermal exposure to NPs can result from medical, cosmetic, industrial, and agricultural products, as well as environmental contamination. The permeability of NPs into and through the skin and their potential toxicity to human health has been recently investigated<sup>12, 13, 14, 15</sup>.

Skin irritation potential and cytotoxic effects of various sizes of nanosilica particles (7 and 10–20 nm) were observed in a cultured human keratinocytes (CHK) model, but no similar observation was found when using a human skin equivalent model (HSEM) with nanosilica concentration at 500 g/ml<sup>16</sup>. Skin permeability and toxicological property of well-dispersed amorphous silica particles for sizes ranging from 70 to 1000 nm was investigated using an in vitro artificial skin model for the penetration assay and in vivo mice model for penetration and toxicity evaluation<sup>17</sup>. The result suggested that decreasing particle size (down to 70 nm) increases NPs skin permeability. Most current studies on the distribution and toxicology of NPs on systems or organs emphasize the liver, kidney, lungs, and GI tract, and skin penetration studies are largely qualitative and sometimes contradictory<sup>18</sup>.

Medical research of iron oxide and silica oxide NPs recently has been focused on quantitative pharmacokinetic studies of systemic circulation and organs such as the liver, kidney, lungs, and GI tract, but minimal quantitative skin absorption and penetration study has been reported to date<sup>14, 2, 3, 4, 5</sup>. Hence, research in skin absorption and penetration of NPs with different physicochemical properties needs to accelerate and gain advanced knowledge.

Here, we studied four metal oxide NPs of varying sizes (12 nm Fe<sub>3</sub>O<sub>4</sub>, 32 nm Fe<sub>3</sub>O<sub>4</sub>@SiO<sub>2</sub>, and 33 nm/78 nm SiO<sub>2</sub>) with carbon-labeling and prepared as aqueous topical dosing formulations to determine in vitro NP binding affinity to the human stratum corneum (SC), permeation capacity into and through human skin layer, and dermatopharmacokinetic analysis. These radiolabeled NP formulations allowed for easy topical application, stability, and accurate measurement. They also possess similarities as well as different physicochemical properties which should provide benefits for skin binding and penetration study.

## **Materials and Methods**

### **Nanoparticle synthesis and characterization**

Four [<sup>14</sup>C]-radiolabeled NP topical formulations, 12 nm Fe<sub>3</sub>O<sub>4</sub> (10 mg/ml water, 24051 DPM/mg particles), 32 nm Fe<sub>3</sub>O<sub>4</sub>@SiO<sub>2</sub> (10 mg/ml water, 1224 DPM/mg particles), 33 nm SiO<sub>2</sub> (10 mg/ml water, 557 DPM/mg particles), and 78 nm SiO<sub>2</sub> (10 mg/ml water, 372 DPM/mg particles) were synthesized, characterized by Oak Ridge National Laboratory (Oak Ridge, TN) and gifted from Lawrence Livermore National Laboratory (Livermore, CA). These NP formulations were individually administered in SC binding, skin penetration, and dermatopharmacokinetic studies without further dilution.

These synthesized NPs were modified with chemically grafted carboxylate groups (-COO-) on surfaces through a previously reported method<sup>19</sup>, and thus the NPs are hydrophilic and stable in aqueous phase. Particle sizes, polydispersity, and zeta potential ( $\zeta$ ) of the NPs were examined with dynamic light scattering (DLS) measurements in deionized water at pH 7.0  $\pm$  0.5 using a NanoBrook 90Plus/PALS (Brookhaven Instruments Corp., Holtsville, NY). NP sizes were also characterized by Hitachi S-4700 scanning electron microscope (SEM) (Hitachi Instruments, Ltd., Tokyo, Japan) and transmission electron microscopy (TEM) (Agilent Technologies, Santa Clara, CA) measurements. Specific radioactivities of the synthesized NPs were measured using a Perkin-Elmer Tri-Carb 2810 TR liquid scintillation counter (LSC) (PerkinElmer Inc., Waltham, MA). Samples were mixed with ULTIMA Gold XR high flash-point LSC-cocktail solution (PerkinElmer Inc., Waltham, MA) for the measurement. Details of the synthesis and characterization have been described in a published patent<sup>20</sup>.

### **Human skin preparations**

The in vitro skin binding and penetration study using human (cadaver and surgical) skin was approved by the UCSF Human Research Committee. Skin samples were freshly dermatomed from 6 human adult cadavers (ages 47 – 78, average 63  $\pm$  12 years, 3 males and 3 females) within 24 hours after death at the

UCSF Anatomy Laboratory. Skin collected from abdominal and thigh regions is normally recommended for in vitro skin exposure assessment and modelling studies since it provides realistic dermal absorption values<sup>21</sup>. Dermatomed skin containing SC, “viable” epidermis, and partial dermis in ~500- $\mu$ m thickness was stored at 0-4 °C for approximately two weeks before being used or further separated to obtain SC membrane.

To ensure the integrity of each skin section, its physical condition was first examined using a 5 - 30X binocular stereo microscope (American Optical Corp., Buffalo, NY) to eliminate any surface damage or potential holes. The thickness of the skin was then measured with an electronic digital caliper (Fisher Scientific, Fair Lawn, NJ). Trans-epidermal water loss (TEWL) from SC was assessed before application of the test formulations. Following a brief (1-2 hours) equilibrium of skin and phosphate-buffered saline, 0.1 M and pH 7.0, each skin sample was measured with a VapoMeter (Delfin Technologies Ltd., Kuopio, Finland). A skin specimen in which the TEWL value was less than 15 g/h m<sup>2</sup> was considered acceptable<sup>22</sup>.

SC membrane, used for in vitro SC binding study, was separated from the above dermatomed skin sample using modified methods of Kassis and S ndergaard<sup>23</sup> and Surber<sup>24</sup>. Briefly, the dermatomed skin was submerged in phosphate-buffered saline (0.05 M, pH 7.2) at 60 °C for 1 min. SC-epidermis layer was then peeled from the dermis with dissection forceps and placed dermal side down on a filter paper soaked with 0.5% trypsin solution (w/w, pH 8.2) at 36 °C for 15 hrs. After incubation, SC-epidermis layer was smoothed out on a flat surface and mushy epidermis removed by firmly rubbing with a moistened cotton-tipped applicator. The SC sheet was rinsed with water three times and then lifted out on a steel wire mesh to dry at 37 °C in an evaporative incubator (Fisher Scientific) overnight. Dry SC was stored in a vacuumed desiccator (Fisher Scientific) at room temperature until use.

### **In vitro stratum corneum binding study**

SC was cut into a 1 cm<sup>2</sup> disc and embedded in 1 mL of dosing solution in a 10-ml glass vial in a shaking water-bath (Fisher Scientific Isotemp Shaking Water Bath) at 37 °C. Binding rates were determined at different incubation times (0.5 hours, 2 hours, 4 hours, and every 4 hours until reaching equilibrium). When the incubation ended, the SC samples were removed and rinsed thrice with 1 mL phosphate buffer saline (PBS, 10 mM, pH 7.4) and all samples were individually measured for radioactivity.

### **In vitro skin penetration study**

Human dermatomed skin samples were placed on a continuous flow-through diffusion cell system (PermeGear, Inc., Hellertown, PA). The donor chamber (above the skin, about 1 cm<sup>2</sup> surface area) remained open to air. The receiving chamber (below the skin, 3 mL in volume) was filled to capacity with receptor fluid, phosphate buffer saline (PBS, 10 mM, pH 7.4), and stirred magnetically at ~600 RPM. PBS was pumped through the diffusion cell at a rate of 4 mL/h using a Pump Pro MPL (Watson-Marlow, Inc., Wilmington, MA). The cell was maintained at approximately 32 °C using a LAUDA heating circulator (LAUDA, Lauda-Königshofen, Germany).

A single dose of 20 µL of each [<sup>14</sup>C]-NP dosing solution was applied to the skin surface (1 cm<sup>2</sup>) and left for 30 minutes or 24 hours. After defined exposure times, skin surface dose residue was immediately washed off with a small piece of cotton pad, wetted once with 5% soap (soft soap, Colgate-Palmolive), twice wetted with water, and finally dried with a cotton pad. All washed samples per skin surface were placed into a glass scintillation vial to quantify radioactivity. Receptor fluid samples were individually collected into glass tubes at defined time points after dose using a Retriever Fraction Collector (Teledyne ISCO, Inc., Lincoln, NE) at 30 and 60 minutes, 2 hours, and then every 2 hours until the end of the experiment at 24 hours.

After a 24-hour experiment finished, the skin was removed from the glass cell and 10 consecutive D-Squame<sup>®</sup> tape strips (CuDerm Corp., Dallas, TX) were performed to remove SC adopted

methods of Rougier<sup>25</sup> and USFDA<sup>26</sup>. The first two stripped samples were counted separately as dose residues. The rest of the tape stripped samples (numbers 3 to 10) were pooled together in a glass scintillation vial. The remaining skin was separated into two parts, epidermis and dermis, using short-period heat contact (60 °C for 2 min) as described by Kassis and Søndergaard<sup>23</sup>. All skin samples were digested by adding 2-5 ml of Soluene-350™ (PerkinElmer Life and Analytical Sciences, Boston, MA) to be liquidized. An aliquot (1 mL) of the receptor fluid samples was collected from each time point for radioactive assay.

### **In vitro dermatopharmacokinetic study**

For dermatopharmacokinetic study, the experiment procedure was similar to that of in vitro skin penetration study. The only differences were: 1) a single dose was applied to the skin surface (1 cm<sup>2</sup>) for 24 hours of dermal exposure, 2) skin surface dose residue was washed off at 24 hours post dose, and 3) after skin washes, the SC surface was tape stripped by 20 consecutive D-Squame® tape strips modified from methods of Weigmann<sup>27</sup> and Leal<sup>28</sup>. The first two stripped samples were counted separately as dose residues. For the rest of the stripped samples (numbers 3 to 20), each was placed individually into a glass scintillation vial to examine NPs distribution in SC.

### **Radioactivity measurements**

Samples were mixed with the Ultima Gold™ scintillation cocktail (PerkinElmer Life and Analytical Sciences, Boston, MA) to measure radioactivity with a PerkinElmer Tri-Carb 2900 TR liquid scintillation spectrometer (Perkin Elmer Life and Analytical Sciences, Downer Grove, IL).

Radioactivity of each sample was adjusted by subtracting background activity. The percentage of applied dose was then calculated by dividing by standard activity of each NP sample and multiplying by 100.

### **Data calculation and analysis**

## Dose calculations

Immediately before and after a single-dose application, a standard dose (20 µl for skin penetration or PK studies, or 1 ml for binding study) was weighed and radioactivity was measured for each formulation.

Weight-normalized standard dose was expressed as radioactivity versus net dose weight (DPM/g standard dose). Based on the ratio of radioactivity and dose weight of the standard dose, radioactivity (DPM) of each individual sample was then calculated from its dose weight and normalized standard dose using the calculation formula below.

Radioactivity per gram weight (DPM/g) of the standard dose × sample dose weight (g) = radioactivity of sample totally dosed (DPM).

Radioactivity recovery of each sample as percent dose applied (% D) was calculated using the formula below.

Sample radioactivity measured (DPM) ÷ radioactivity of sample totally dosed × 100% = radioactivity recovery of sample dose as percent dose applied (% D).

## Data analysis

Individual and mean (± S.D.) amounts of test NP equivalent in the SC, epidermis, dermis, receptor fluid, and wash samples are presented as percent administered dose at each time point. Binding rates were determined after reaching equilibrium, approximately in 20 hour post.

Dermatopharmacokinetic analysis was performed with SigmaPlot (v13, Systat Software, Inc., San Jose, CA) for logarithm curve fitting.

Statistical difference of each NP between short (30-minute) surface exposure and long exposure (24-hour) was tested by Student T-test with SigmaStat (v3.0, Systat Software, Inc., San Jose, CA).

Significance was defined as P value ≤ 0.05.

## Results

Table 1 provides the physical characteristics of the four synthesized NP samples. The NPs used in this research are surface-functionalized by carboxylate groups, thus they have hydrophilic surfaces and only effects from NPs of a hydrophilic nature were examined, as noted in the text description. Particle sizes, polydispersity, and zeta potential ( $\zeta$ ) of the NPs were examined with dynamic light scattering (DLS) measurements in deionized water at pH  $7.0 \pm 0.5$  using a Brookhaven 90Plus/PALS instrument. NP sizes were also characterized by SEM and TEM. Specific radioactivity of the NPs was measured by a liquid scintillation analyzer.

Table 2 summarizes binding affinity of the four NP samples to SC after reaching equilibrium (20 – 24 hours post incubation). Binding rates of SC to the NPs quickly reached 90% or more of its capacity 30 minutes post dosing/incubation, and then slowly increased to equilibrium at approximately 20 hours. We thus used the binding rate at 24 hours as SC maximum binding capacity for these four NPs. [ $^{14}\text{C}$ ]- $\text{Fe}_3\text{O}_4@ \text{SiO}_2$  NP (32 nm) has the highest binding rate, followed by [ $^{14}\text{C}$ ]- $\text{Fe}_3\text{O}_4$  NP (12 nm) and [ $^{14}\text{C}$ ]- $\text{SiO}_2$  (78 nm). [ $^{14}\text{C}$ ]- $\text{SiO}_2$  (33 nm) has the lowest binding rate.

Table 3 explores the effect of a short dermal exposure (30 min) on penetration and distribution of four NPs in skin layers – SC, epidermis, and dermis, as well as receptor fluid. [ $^{14}\text{C}$ ]- $\text{Fe}_3\text{O}_4$  NPs (12 nm) permeated into SC ( $1.0\% \pm 0.4$ ) and epidermis ( $1.1\% \pm 0.6$ ), but were not found in dermis and receptor fluid (RF). [ $^{14}\text{C}$ ]- $\text{Fe}_3\text{O}_4@ \text{SiO}_2$  NPs (32 nm) were only detected in SC ( $3.2\% \pm 2.7$ ), but not found in epidermis, dermis, and RF. No evidence of skin absorption/penetration was observed for the other two NPs, [ $^{14}\text{C}$ ]- $\text{SiO}_2$  (33 nm) and [ $^{14}\text{C}$ ]- $\text{SiO}_2$  (78 nm).

Table 4 further demonstrates that after extending dermal exposure time to 24 hours, all NPs permeated SC but only [ $^{14}\text{C}$ ]- $\text{Fe}_3\text{O}_4$  NPs (12 nm) were in both SC ( $0.4\% \pm 0.1$ ) and epidermis ( $0.1\% \pm 0.1$ ). No NPs were found in the dermis and receptor fluid collected at 24 hours.

SC penetration kinetics of the NPs was studied using the in vitro SC tape stripping method. Twenty-four hours post topical application, tested skin was tape stripped 20 times to remove approximately 50% of SC by thickness, and the results represent the distribution of NPs in SC layer. [<sup>14</sup>C]-Fe<sub>3</sub>O<sub>4</sub> NPs (12 nm) were observed as deep as 50% of SC layer in depth (Figure 1), while 32 nm Fe<sub>3</sub>O<sub>4</sub>@SiO<sub>2</sub> NPs were mostly found in the first 10 strips (Figure 2). The 33 nm and 78 nm SiO<sub>2</sub> NPs, however, were only found in the first four tape strips. In general, test substance retained in the top few layers of SC (i.e. contained in the first few tape strips) may be removed by desquamation and therefore may not be absorbed systemically<sup>29, 30</sup>. We therefore concluded that no actual SC absorption/penetration was present for two SiO<sub>2</sub> NPs (Figures 3 and 4).

## Discussion

This study demonstrated that 12 nm Fe<sub>3</sub>O<sub>4</sub> NPs penetrated into SC and through to viable epidermis (Table 3) 30 minutes post dermal exposure, while other larger sizes of NPs (32 nm Fe<sub>3</sub>O<sub>4</sub>@SiO<sub>2</sub> or 33 nm and 78 nm SiO<sub>2</sub>) needed much longer exposure times (24 hours) to partition into SC (Table 4) but not in the epidermis. The NPs' size differences contributed to these variations in their permeability. Similar observations were reported by Baroli<sup>31</sup> and Rouse<sup>32</sup> that only when NP size is small enough, such as when iron oxide size is 10 nm or less, is it possible to diffuse through the SC to the epidermis<sup>31</sup>. Thus, NP size is an important factor in determination of SC permeability.

Size dependent NP penetration is not only observed in normal integrity skin, but also in disrupted SC. Effect of partial SC disruption on silica oxide NPs (40 nm size or larger) penetration was tested after cyanacrylate skin surface stripping (CSSS) pretreatment<sup>33</sup>, or CSSS pretreatment plus positive or negative surface charging as skin penetration promotion<sup>7</sup>. Results indicated that even when SC barrier structure was partially disrupted, only 40 nm silica oxide NPs were found in epidermal Langerhans cells (LC), and no larger sizes of silica NPs penetrated into the epidermis<sup>7, 33</sup>. The results further emphasized the importance of NP size in determination of skin (deep) penetration even when the skin barrier has been disrupted.

NP size however may not be the only factor in determining SC permeability. Two structurally different NPs Fe<sub>3</sub>O<sub>4</sub>@SiO<sub>2</sub> and SiO<sub>2</sub> had similar sizes 32 nm and 33 nm, respectively, but showed different SC penetration rates. When they were topically dosed on the skin in vitro for 24 hours, total SC penetration (% dose) of 32 nm Fe<sub>3</sub>O<sub>4</sub>@SiO<sub>2</sub> was four times that of 33 nm SiO<sub>2</sub> (Table 4). This result demonstrated that NPs' structurally related physicochemical property variation could result in different skin permeability.

NPs' structural variations also change their SC binding rates. The main barrier function of the skin is dominated by protein (keratin, 70 – 80%) and lipids<sup>34</sup>. Chemicals' binding affinities to SC protein/lipids are associated with their skin permeability<sup>35</sup>. As shown in Table 2 after 24 hours of incubation, SC binding rate of 32 nm Fe<sub>3</sub>O<sub>4</sub>@SiO<sub>2</sub> was also four times of that of 33 nm SiO<sub>2</sub>. The results suggest that iron oxide NPs have higher SC affinity than that of silica oxide NPs. Thus, determination of the SC binding affinity of NPs may be a useful method to estimate NP diffusion in SC.

SC has heterogeneous structure composed of 15 – 20 layers of flattened corneocytes embedded in lipid bilayers<sup>36</sup>. SC tape stripping method measures SC mass, absorption, reservoir and pharmacokinetics of testing chemicals in a defined exposure period<sup>37, 38</sup>.

Tables 3 and 4 provided information of radioactivity recovery of total SC absorbance for each tested NP (% dose) after pooling together all stripped samples to count. The results demonstrated that NP size is an important factor in determination of SC permeability and extension of exposure did not significantly alter the permeability of these NPs ( $P \geq 0.05$ ).

Figures 1 to 4 emphasized NP distribution in the SC presented by individual tape-stripped sample after a 24-hour exposure. These continuously collected SC stripped samples gave the concentration profile of a NP in SC in relation to the relative SC depth.

Small size Fe<sub>3</sub>O<sub>4</sub> NPs (12 nm) reached approximately 40-60% of whole SC thickness while larger 32 nm Fe<sub>3</sub>O<sub>4</sub>@SiO<sub>2</sub> was approximately 20% deep (Figures 1 & 2). This further supports the importance of NP size in skin penetration. However compared to 32 nm Fe<sub>3</sub>O<sub>4</sub>@SiO<sub>2</sub>, 33 nm SiO<sub>2</sub> only reached the superficial layers of the SC (Figure 3) and showed no difference compared to 78 nm SiO<sub>2</sub> (Figure 4). This may be explained by NPs' SC binding affinity.

Based on structural and functional differences, SC can be further divided into three layers. The superficial layer (0-30% SC depth) of SC has highly folded keratin filaments, which are loosely bound to

outer corneocytes to allow chemicals to pass quickly during influx and efflux, and retaining<sup>39,40</sup>. Thus, the initial tape strips removed higher amounts of SC protein and retained testing chemicals. The intermediate (30-70%) and the bottom (80-100%) layers exhibited distinct barrier properties to chemical permeation. The major difference is that the former has unfolded keratin filaments and the most water binding, while in the latter the water binding sites are already occupied with water and cannot swell substantially<sup>39,40</sup>. Thus, the quantity of SC removed by tape stripping is not linearly proportional to the number of tape strips removed and the values progressively decreased as the tape number increased. As illustrated by Figures 1 to 4, whether or not these NPs penetrated into the low part of the SC, they were present in high amount in the superficial layer of the SC and then quickly or slowly declined.

Knowledge of the concentration profile of a NP or chemical in SC in relation to the relative SC depth is important to predict its permeation status, whether it will desquamate, retain, or further diffuse to systemic. The superficial layer of SC is involved in the process of desquamation, therefore the amount of chemical found in this layer is usually not considered as skin absorbed. Chemicals retained in the intermediate and bottom layers, however, might further penetrate into the deep tissues or systemic<sup>41</sup>.

The relation between the number of tape strips and SC depth (relative thickness of the horny layer) can be used to estimate chemical penetration and distribution in SC, in which the total absorbance corresponds to cumulated values of pseudo-absorption of all removed tape strips. Based on this relation, the relative amount of SC stripped with each tape can be calculated in terms of the percentage of SC thickness<sup>42,43</sup>. For example the range of relative SC removed (%) by 20 tape strips can be from 40 to 60% depending upon variations of the test chemical and vehicle used and the skin sample's regional and physical variations<sup>37,44</sup>.

In conclusion, this study confirmed that NP size is an important factor affecting percutaneous absorption of NPs. Only when Fe<sub>3</sub>O<sub>4</sub> NP size was 12 nm could it reach the epidermis while other larger sizes of NPs (Fe<sub>3</sub>O<sub>4</sub>@SiO<sub>2</sub> NP and silica NPs) were only retained in SC. Even with the exposure extended from 30 min to 24 hours, penetration was not enhanced. Binding rates of these NPs to SC were similar to the amounts of the NPs retained in SC after a 24-hour dermal exposure. Iron oxide NPs had relatively higher binding rates to SC compared to those of silica oxide NPs. The relationship of these NPs to skin was further demonstrated by in vitro dermatopharmacokinetic analysis using SC tape stripping method, which gave a clear illustration of NPs. The binding affinity determination may be a useful method to quickly screen skin penetration of NPs.

At this point, we await confirmation of these results with in vivo studies – evaluating not only the skin penetration effect of different NPs with various particle sizes, but also related permeation kinetics as well.

### **Acknowledgement**

This research is supported by Defense Threat Reduction Agency (DTRA) Grant: HDTRA1-14-0005 UCSF (BRBAA11-PerC-9-2-0054 –Base).

## References

- 1 Baroli B. Penetration of nanoparticles and nanomaterials in the skin: fiction or reality? *J Pharm Sci.* 2010; **99**(1):21-50.
- 2 Shao D, Wang Z, Dong WF, Zhang X, Zheng X, Xiao XA, Wang YS, Zhao X, Zhang M, Li J, Huo QS, Chen L. Facile Synthesis of Core-shell Magnetic Mesoporous Silica Nanoparticles for pH-sensitive Anticancer Drug Delivery. *Chem Biol Drug Des.* 2015; **86**(6):1548-53.
- 3 Popescu S, Ardelean IL, Gudovan D, Rădulescu M, Fikai D, Fikai A, Vasile BŞ, Andronescu E. Multifunctional materials such as MCM-41÷Fe3O4÷folic acid as drug delivery system. *Rom J Morphol Embryol.* 2016; **57**(2):483-9.
- 4 Graf C, Meinke M, Gao Q, Hadam S, Raabe J, Sterry W, Blume-Peytavi U, Lademann J, Rühl E, Vogt A. Qualitative detection of single submicron and nanoparticles in human skin by scanning transmission x-ray microscopy. *J Biomed Opt.* 2009; **14**(2):021015.
- 5 Zhou F, Teng F, Deng P, Meng N, Song Z, Feng R. Recent Progress of Nano-drug Delivery System for Liver Cancer Treatment. *Anticancer Agents Med Chem.* 2018; **17**(14):1884-1897.
- 6 European Commission, Departments and Service, Public Health: Nanotechnologies-Level 2-Question 6. 2006.  
[http://ec.europa.eu/health/scientific\\_committees/opinions\\_layman/en/nanotechnologies/l-2/6-health-effects-nanoparticles.htm](http://ec.europa.eu/health/scientific_committees/opinions_layman/en/nanotechnologies/l-2/6-health-effects-nanoparticles.htm). (accessed 21 June 2019).
- 7 Rancan F, Gao Q, Graf C, Troppens S, Hadam S, Hackbarth S, Kembuan C, Blume-Peytavi U, Rühl E, Lademann J, Vogt A. Skin penetration and cellular uptake of amorphous silica nanoparticles with variable size, surface functionalization, and colloidal stability. *ACS Nano.* 2012; **6**(8):6829-42.

- 8 Sapsford KE, Algar WR, Berti L, Gemmill KB, Casey BJ, Oh E, Stewart MH, Medintz IL. Functionalizing nanoparticles with biological molecules: developing chemistries that facilitate nanotechnology. *Chem Rev.* 2013; **113**(3):1904-2074.
- 9 Gwinn MR and Vallyathan V. Nanoparticles: Health Effects—Pros and Cons. *Environ Health Perspect.* 2006; **114**(12): 1818–1825.
- 10 Meglio PD, Perera GK, Nestle FO. The Multitasking Organ: Recent Insights into Skin Immune Function. *Immunity.* 2011; **35**(16):857–869.
- 11 Boer M, Duchnik E, Maleszka R, Marchlewicz M. Structural and biophysical characteristics of human skin in maintaining proper epidermal barrier function. *Postepy Dermatol Alergol.* 2016; **33**(1): 1–5.
- 12 Liang XW, Xu ZP, Grice J, Zvyagin AV, Roberts MS, Liu X. Penetration of nanoparticles into human skin. *Curr Pharm Des.* 2013; **19**(35):6353-66.
- 13 Watkinson AC, Bunge AL, Hadgraft J, Lane ME. Nanoparticles do not penetrate human skin—a theoretical perspective. *Pharm Res.* 2013; **30**(8):1943-6.
- 14 Lin Z, Monteiro-Riviere NA, Riviere JE. Pharmacokinetics of metallic nanoparticles. *Wiley Interdiscip Rev Nanomed Nanobiotechnol.* 2015; **7**(2):189-217.
- 15 Gupta R and Rai B. Penetration of Gold Nanoparticles through Human Skin: Unraveling Its Mechanisms at the Molecular Scale. *J. Phys. Chem. B,* 2016; **120**(29): 7133–7142.
- 16 Park YH, Kim JN, Jeong SH, Choi JE, Lee SH, Choi BH, Lee JP, Sohn KH, Park KL, Kim MK, Son SW. Assessment of dermal toxicity of nanosilica using cultured keratinocytes, a human skin equivalent model and an in vivo model. *Toxicology.* 2010; **267**(1-3):178-81.
- 17 Matsuo K, Hirobe S, Okada N, Nakagawa S. Analysis of Skin Permeability and Toxicological Properties of Amorphous Silica Particles. *Biol Pharm Bull.* 2016; **39**(7):1201-5

- 18 Schneider M, Stracke F, Hansen S, Schaefer UF. Nanoparticles and their interactions with the dermal barrier. *Dermatoendocrinol.* 2009; **1**(4):197-206.
- 19 Wang W, Nallathamby PD, Foster CM, Morrell-Falvey JL, Mortensen NP, Doktycz MJ, Gu B, Retterer ST. Volume labeling with Alexa Fluor dyes and surface functionalization of highly sensitive fluorescent silica (SiO<sub>2</sub>) nanoparticles, *Nanoscale*, 2013; **5**(21): 10369-10375.
- 20 Wang W, Gu B, Retterer ST, Doktycz MJ. Volume-labeled nanoparticles and methods of preparation, US Patent 9,011,735, 2015. <https://www.osti.gov/biblio/1178265-volume-labeled-nanoparticles-methods-preparation>. (accessed 21 June 2019).
- 21 EFSA (European Food Safety Authority): Guidance on Dermal Absorption. *EFSA Journal* 2012; **10**(4):2665. <http://onlinelibrary.wiley.com/doi/10.2903/j.efsa.2012.2665/epdf>. (accessed 21 June 2019).
- 22 De Paepe K, Houben E, Adam R, Wiesemann F, Rogiers V. Validation of the VapoMeter, a closed unventilated chamber system to assess transepidermal water loss vs. the open chamber Tewameter. *Skin Res Technol.* 2005; **11**(1):61-9.
- 23 Kassis V, Søndergaard J. Heat-separation of normal human skin for epidermal and dermal prostaglandin analysis. *Arch Dermatol Res.* 1982; **273**(3-4):301-6
- 24 Surber C, Wilhelm KP, Maibach HI, Hall LL, Guy RH. Partitioning of chemicals into human stratum corneum: implications for risk assessment following dermal exposure. *Fundam Appl Toxicol.* 1990; **15**(1):99-107.
- 25 Rougier A, Dupuis D, Lotte C & Maibach HI. Chat: Stripping method for measuring percutaneous absorption in vivo. In: Bronaugh RL & Maibach HI eds. *Percutaneous absorption: drugs–cosmetics–mechanisms–methodology*, 3rd ed. New York, Marcel Dekker, pp 375–393, 1999 (*Drugs and the Pharmaceutical Sciences Vol. 97*).

- 26 USFDA: Guidance for industry: topical dermatological drug product NDAs and ANDAs — in vivo bioavailability, bioequivalence, in vitro release, and associated studies. Draft guidance, June 1998. Rockville, MD, United States Department of Health and Human Services, Food and Drug Administration, Center for Drug Evaluation and Research.  
<https://www.govinfo.gov/content/pkg/FR-2002-05-17/pdf/02-12326.pdf>. (accessed 21 Jun 2019).
- 27 Weigmann H, Lademann J, Pelchrzim R, Sterry W, Hagemeister T, Molzahn R, Schaefer M, Lindscheid M, Schaefer H, Shah VP. Bioavailability of clobetasol propionate-quantification of drug concentrations in the stratum corneum by dermatopharmacokinetics using tape stripping. *Skin Pharmacol Appl Skin Physiol*. 1999; **12**(1-2):46-53.
- 28 Leal LB, Cordery SF, Delgado-Charro MB, Bunge AL, Guy RH. Bioequivalence Methodologies for Topical Drug Products: In Vitro and Ex Vivo Studies with a Corticosteroid and an Anti-Fungal Drug. *Pharm Res*. 2017; **34**(4):730-737.
- 29 OECD GUIDANCE NOTES ON DERMAL ABSORPTION, 22 Oct 2010.  
<http://www.oecd.org/chemicalsafety/testing/46257610.pdf>. (accessed 21 June 2019).
- 30 Niazi S. CH 10 Topical drugs, in *Handbook of bioequivalence testing*, ed by Sarfaraz K. Niazi. 2nd Ed. New York, CRC Press, pp285-292, 2015.
- 31 Baroli B, Ennas MG, Loffredo F, Isola M, Pinna R, López-Quintela MA. Penetration of metallic nanoparticles in human full-thickness skin. *J Invest Dermatol*. 2007; **127**(7):1701-12.
- 32 Rouse JG, Yang J, Ryman-Rasmussen JP, Barron AR, Monteiro-Riviere NA. Effects of mechanical flexion on the penetration of fullerene amino acid-derivatized peptide nanoparticles through skin. *Nano Lett*. 2007; **7**(1):155-60.

- 33 Vogt A, Combadiere B, Hadam S, Stieler KM, Lademann J, Schaefer H, Aufran B, Sterry W, Blume-Peytavi U. 40 nm, but not 750 or 1,500 nm, nanoparticles enter epidermal CD1a+ cells after transcutaneous application on human skin. *J Invest Dermatol.* 2006; **126**(6):1316-22.
- 34 Benson HAE. Skin structure, function, and permeation. In: Benson HAE, Watkinson AC, editors. *Topical and transdermal drug delivery: Principles and practice.* New Jersey: Jhon Wiley & Sons, Inc.; 2012. p. 3-22
- 35 Cao Y, Elmahdy A, Zhu H, Hui X, Maibach H. Binding affinity and decontamination of dermal decontamination gel to model chemical warfare agent simulants. *J Appl Toxicol.* 2018; **38**(5):724-733.
- 36 Elias PM, Wakefield JS. An integrated view of the epidermal environmental interface. *Dermatologica Sinica.* 2015; **33**(2): 49-57.
- 37 Bashir SJ, Chew AL, Anigbogu A, Dreher F, Maibach HI. Physical and physiological effects of stratum corneum tape stripping. *Skin Res Technol.* 2001; **7**(1):40-8.
- 38 Herkenne C, Naik A, Kalia YN, Hadgraft J, Guy RH. Pig Ear Skin ex Vivo as a Model for in Vivo Dermatopharmacokinetic Studies in Man. *Pharmaceutical Research,* 2006; **23**(8):1850–56.
- 39 Kubo A, Ishizaki I, Kubo A, Kawasaki H, Nagao K, Ohashi Y, Amagai M. The stratum corneum comprises three layers with distinct metal-ion barrier properties. *Sci Rep.* 2013; **3**:1731.
- 40 Choe CS, Schleusener J, Lademann J, Darvin ME. Keratin-water-NMF interaction as a three layer model in the human stratum corneum using in vivo confocal Raman microscopy. *Sci Rep.* 2017; **7**:15900.

- 41 OECD GUIDELINE FOR THE TESTING OF CHEMICALS Skin Absorption: in vitro Method #428, 13 April 2004, <https://ntp.niehs.nih.gov/iccvam/suppdocs/feddocs/oced/ocedtg428-508.pdf>. (accessed 21 June 2019).
- 42 Lindemann U, Wilken K, Weigmann HJ, Schaefer H, Sterry W, Lademann J. Quantification of the horny layer using tape stripping and microscopic techniques. *J Biomed Opt.* 2003; **8**(4):601-7.
- 43 Jacobi U, Weigmann HJ, Ulrich J, Sterry W, Lademann J. Estimation of the relative stratum corneum amount removed by tape stripping. *Skin Res Technol.* 2005; **11**(2):91-6.
- 44 Raj N, Voegeli R, Rawlings AV, Gibbons S, Munday MR, Summers B, Lane ME. Variation in stratum corneum protein content as a function of anatomical site and ethnic group. *Int J Cosmet Sci.* 2016; **38**(3):224-31.

**Table 1. Size, zeta potential, and specific radioactivity of synthesized <sup>14</sup>C-labeled nanoparticles\***

Nanoparticles	SEM (nm) ± deviation	Size (nm) ± polydispersity	ζ (mV) ± half width	Specific radioactivity μCi/μg
<sup>14</sup> C-SiO <sub>2</sub>	33 ± 2.9	42.3 ± 8.8%	-54.6 ± 3.8	0.25
<sup>14</sup> C-SiO <sub>2</sub>	78 ± 4.8	95.6 ± 9.2%	-52.4 ± 3.1	0.17
<sup>14</sup> C-Fe <sub>3</sub> O <sub>4</sub>	12 ± 3.9	47.7 ± 11.9	-24.7 ± 4.3	10.8
<sup>14</sup> C-Fe <sub>3</sub> O <sub>4</sub> @SiO <sub>2</sub>	32 ± 3.3	66.5 ± 15.3	-38.2 ± 2.9	0.51

Physical characteristics of the four synthesized NP samples. The nanoparticles used in this research are surface-functionalized by carboxylate groups, thus they have hydrophilic surfaces and only effects from NPs of a hydrophilic nature were examined, as noted in the text description.

Particle sizes, polydispersity, and zeta potential (ζ) of the NPs were examined with dynamic light scattering (DLS) measurements in deionized water at pH 7.0 ± 0.5 using a Brookhaven 90Plus/PALS instrument. Nanoparticle sizes were also characterized by SEM and TEM. Specific radioactivity of the NPs was measured by a liquid scintillation analyzer. \*Data provided by Oak Ridge National Laboratory, Oak Ridge, TN

**Table 2. Stratum corneum binding affinity (as percent of applied dose) of four nanoparticles after reaching equilibrium**

	<b>Stratum corneum binding affinity (% Dose) after reaching equilibrium</b>			
	12 nm Fe <sub>3</sub> O <sub>4</sub>	32 nm Fe <sub>3</sub> O <sub>4</sub> @SiO <sub>2</sub>	33 nm SiO <sub>2</sub>	78 nm SiO <sub>2</sub>
Stratum corneum	33% ± 4.5	58% ± 2.0	14% ± 2.9	23% ± 2.4

Binding rates of the SC sheet to four NPs were determined at different incubation times (0.5 hours, 2 hours, 4 hours, and every 4 hours until reaching equilibrium). The rates quickly reached 90% of its capacity in 30 minutes post dosing/incubation, and then slowly increased to the maximum value around 20 – 24 hours. The SC sheet was then washed three times followed by counting radioactivity of each fraction. The results indicated the stratum corneum binding affinity for each type of NP. Each number represents the mean ± SD of 6 samples of percent applied dose (% D).

**Table 3. Radioactivity as percentage of applied dose of four NP samples following a 30-minute dermal exposure *in vitro***

	<b>Radioactivity as percentage of applied dose of four NP samples following a 30-minute dermal exposure <i>in vitro</i></b>			
	<b>12 nm Fe<sub>3</sub>O<sub>4</sub></b>	<b>32 nm Fe<sub>3</sub>O<sub>4</sub>@SiO<sub>2</sub></b>	<b>33 nm SiO<sub>2</sub></b>	<b>78 nm SiO<sub>2</sub></b>
Surface residue	97.5% ± 3.3	80.0% ± 11.4	97.4 ± 6.4	91.6% ± 2.6
Stratum corneum	1.0% ± 0.4	3.2% ± 2.7	0%	0%
Epidermis	1.1% ± 0.6	0%	0%	0%
Dermis	0%	0%	0%	0%
Receptor fluid	0%	0%	0%	0%
Mass balance	99.6% ± 3.3	83.2% ± 8.9	97.4% ± 6.4	91.6% ± 2.6

Human skin absorption/penetration studies were conducted on a flow-through diffusion system. Each number represents the mean ± SD of 6 samples. Iron NPs (12 nm and 32 nm) were observed in SC but not SiO<sub>2</sub> NPs. Small iron particles (12 nm Fe<sub>3</sub>O<sub>4</sub> NPs) were found in the epidermal layer.

**Table 4. Radioactivity as percentage of applied dose of four NP samples following a 24-hour dermal exposure *in vitro***

	<b>Radioactivity as percentage of applied dose of four NP samples following a 24-hour dermal exposure <i>in vitro</i></b>			
	<b>12 nm Fe<sub>3</sub>O<sub>4</sub></b>	<b>32 nm Fe<sub>3</sub>O<sub>4</sub>@SiO<sub>2</sub></b>	<b>33 nm SiO<sub>2</sub></b>	<b>78 nm SiO<sub>2</sub></b>
Surface residue	91.9% ± 9.4	94.3% ± 3.6	90.0% ± 8.6	98.9% ± 6.9
Stratum corneum	0.4% ± 0.2	0.9% ± 0.2	0.2% ± 0.2	0.3% ± 0.2
Epidermis	0.1% ± 0.2	0%	0%	0%
Dermis	0%	0%	0%	0%
Receptor fluid	0%	0%	0%	0%
Mass balance	92.5% ± 9.3	95.2% ± 3.9	90.4% ± 8.6	99.2% ± 7.1

Human skin absorption/penetration studies were conducted on a flow-through diffusion system. Each number represents the mean ± SD of 6 samples. After extending dermal exposure time from 30 min. to 24 hours, all four tested NPs were observed in the SC layer in very small quantities but only small iron particles (12 nm Fe<sub>3</sub>O<sub>4</sub> NPs) were found in the epidermal layer.

Figure 1. Dermatopharmacokinetic analysis of Fe<sub>3</sub>O<sub>4</sub> (12 nm) nanoparticles.

Human skin was exposed to testing NPs for 24 hours and then SC samples were collected via 20 consecutive D-Squame® tape strips. The first two stripped samples were considered as unabsorbed dose residues. Number 3 to 20 stripping samples (total 18) were measured individually to examine NPs distribution in SC. Small size (12 nm) Fe<sub>3</sub>O<sub>4</sub> NPs are easily to penetrate into the SC layer. Solid square symbol: individual observed, line: calculated. Each number represents the mean ± SD of 5 samples.

Figure 2. Dermatopharmacokinetic analysis of  $\text{Fe}_3\text{O}_4 @\text{Si}_2$  (32 nm) nanoparticles.

Human skin was exposed to testing NPs for 24 hours and then SC samples were collected via 20 consecutive D-Squame® tape strips. The first two stripped samples were considered as unabsorbed dose residues. Number 3 to 20 stripping samples (total 18) were measured individually to examine NPs distribution in SC. Enlarging particle size to 32 nm,  $\text{Fe}_3\text{O}_4 @\text{Si}_2$  NPs reduced the amount to penetrate into the SC layer. Solid square symbol: individual observed, line: calculated. Each number represents the mean  $\pm$  SD of 5 samples.

Figure 3. Dermatopharmacokinetic analysis of SiO<sub>2</sub> (33 nm) nanoparticles.

Human skin was exposed to testing NPs for 24 hours and then SC samples were collected via 20 consecutive D-Squame® tape strips. The first two stripped samples were considered as unabsorbed dose residues. Number 3 to 20 stripping samples (total 18) were measured individually to examine NPs distribution in SC. Particle size (33 nm) SiO<sub>2</sub> NPs are mostly retained in the superficial layers of the SC (Numbers 3 – 6 of tape strips). Solid circle symbol: individual observed, line: calculated. Each number represents the mean ± SD of 5 samples.

Figure 4. Dermatopharmacokinetic analysis of SiO<sub>2</sub> (78 nm) nanoparticles.

Human skin was exposed to testing NPs for 24 hours and then SC samples were collected via 20 consecutive D-Squame® tape strips. The first two stripped samples were considered as unabsorbed dose residues. Number 3 to 20 stripping samples (total 18) were measured individually to examine NPs distribution in SC. Particle size (78 nm) SiO<sub>2</sub> NPs are mostly retained in the superficial layers of the SC (Numbers 3 – 6 of tape strips). Solid circle symbol: individual observed, line: calculated. Each number represents the mean ± SD of 5 samples.

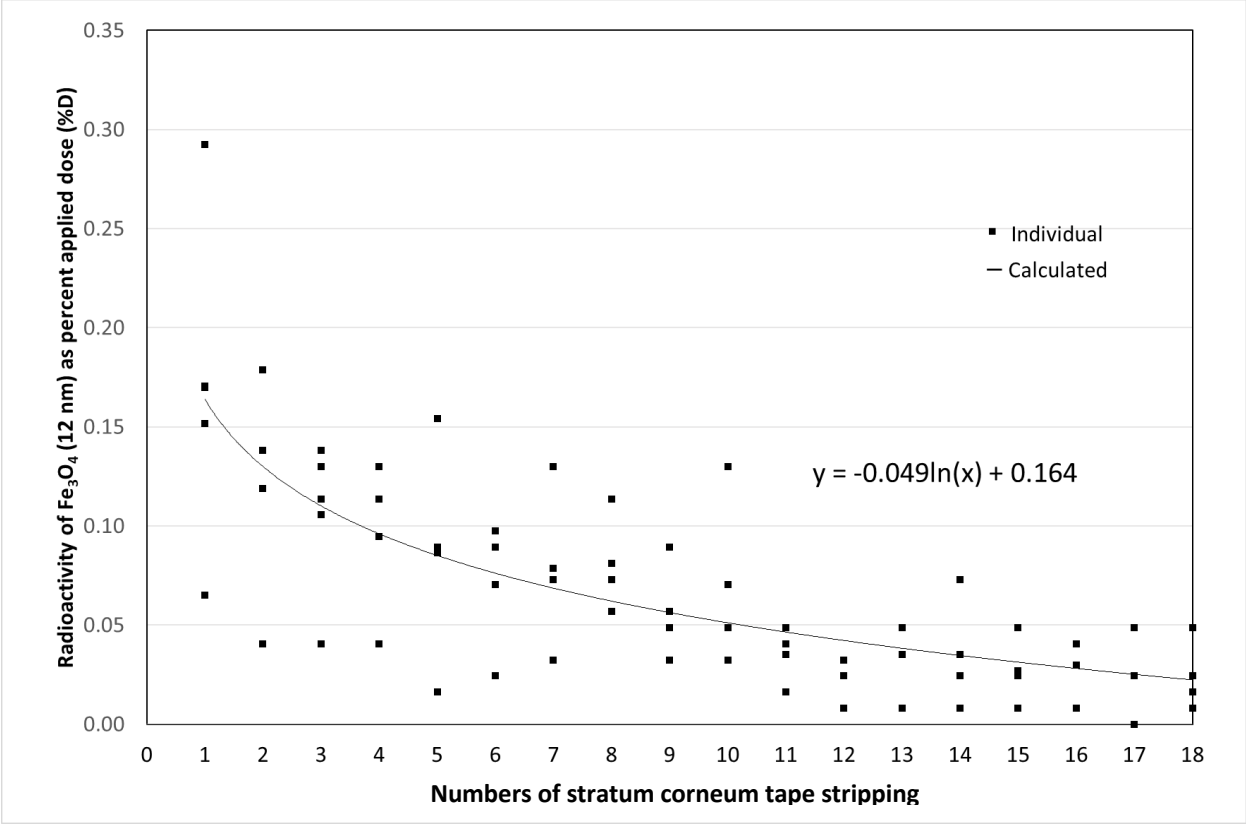


Figure 1. Dermatopharmacokinetic analysis of Fe<sub>3</sub>O<sub>4</sub> (12 nm) nanoparticles.

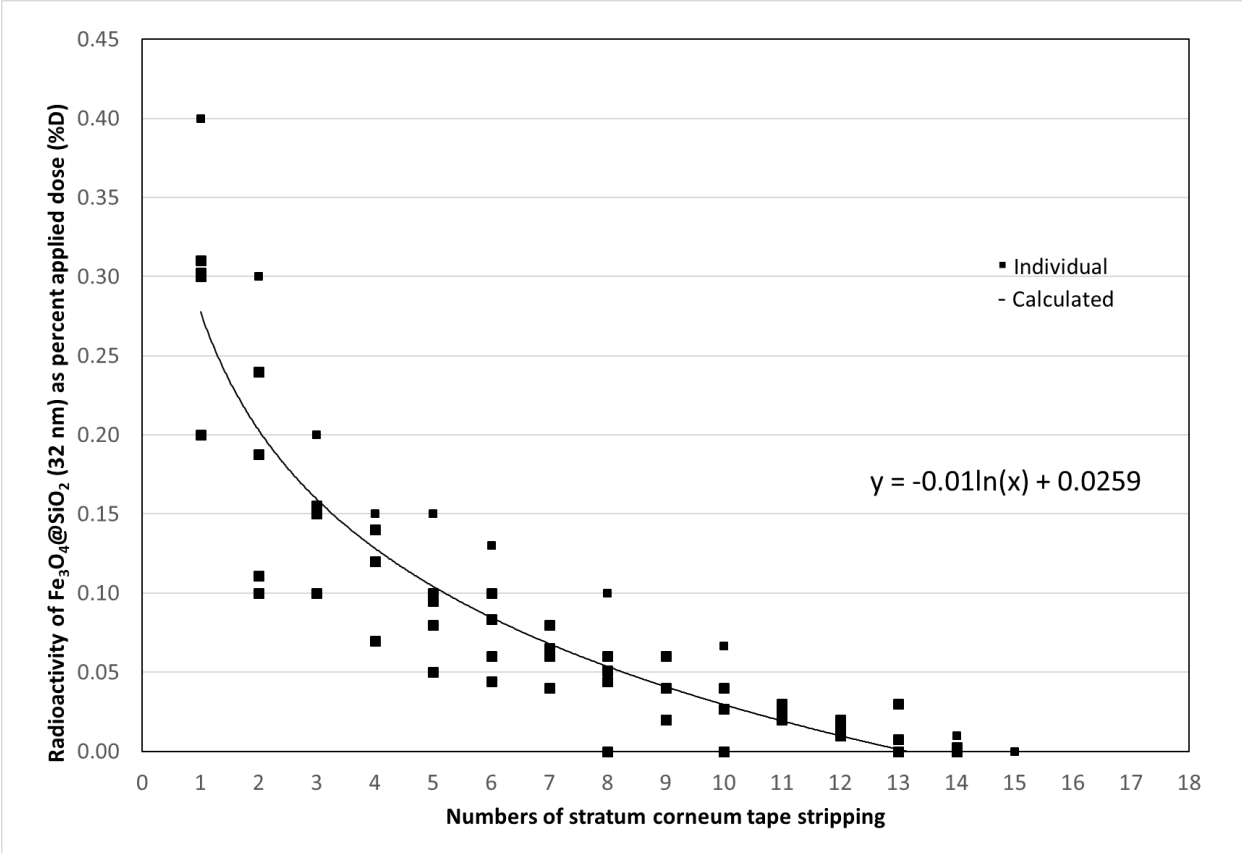


Figure 2. Dermatopharmacokinetic analysis of Fe<sub>3</sub>O<sub>4</sub>@Si<sub>2</sub> (32 nm) nanoparticles.

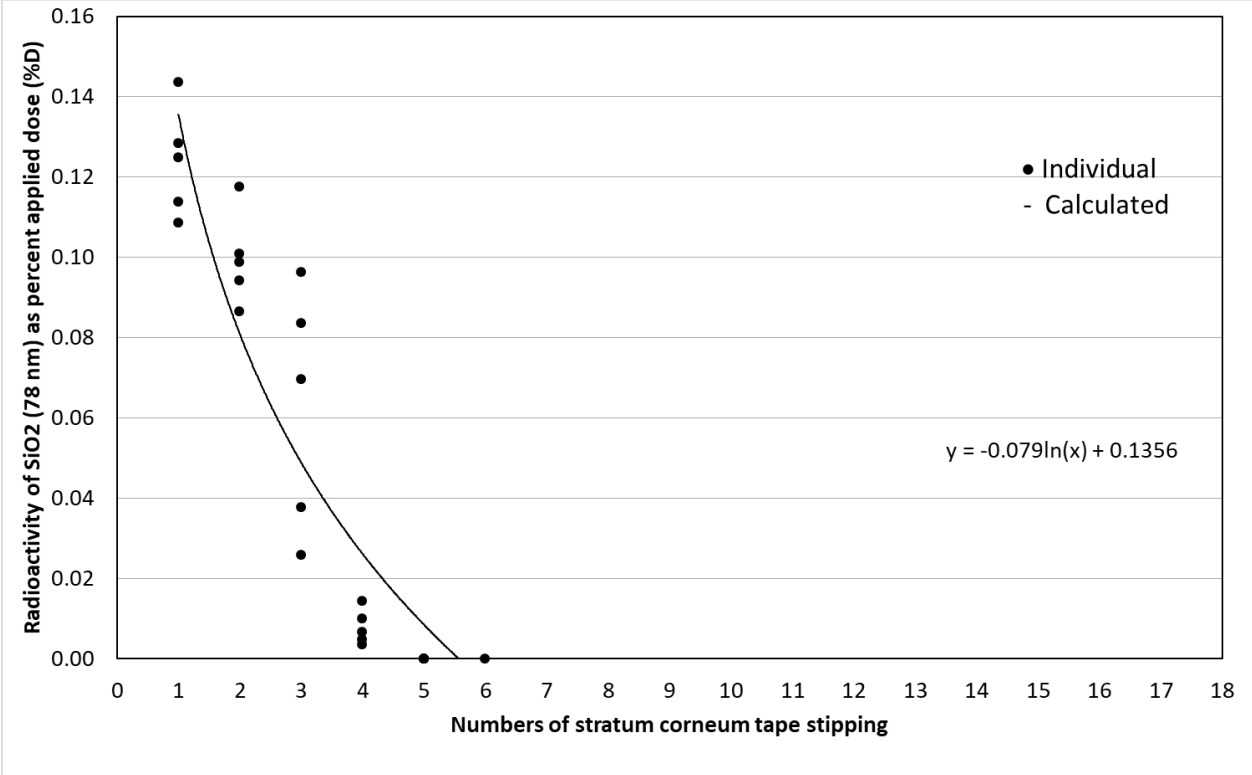


Figure 3. Dermatopharmacokinetic analysis of SiO<sub>2</sub> (33 nm) nanoparticles.

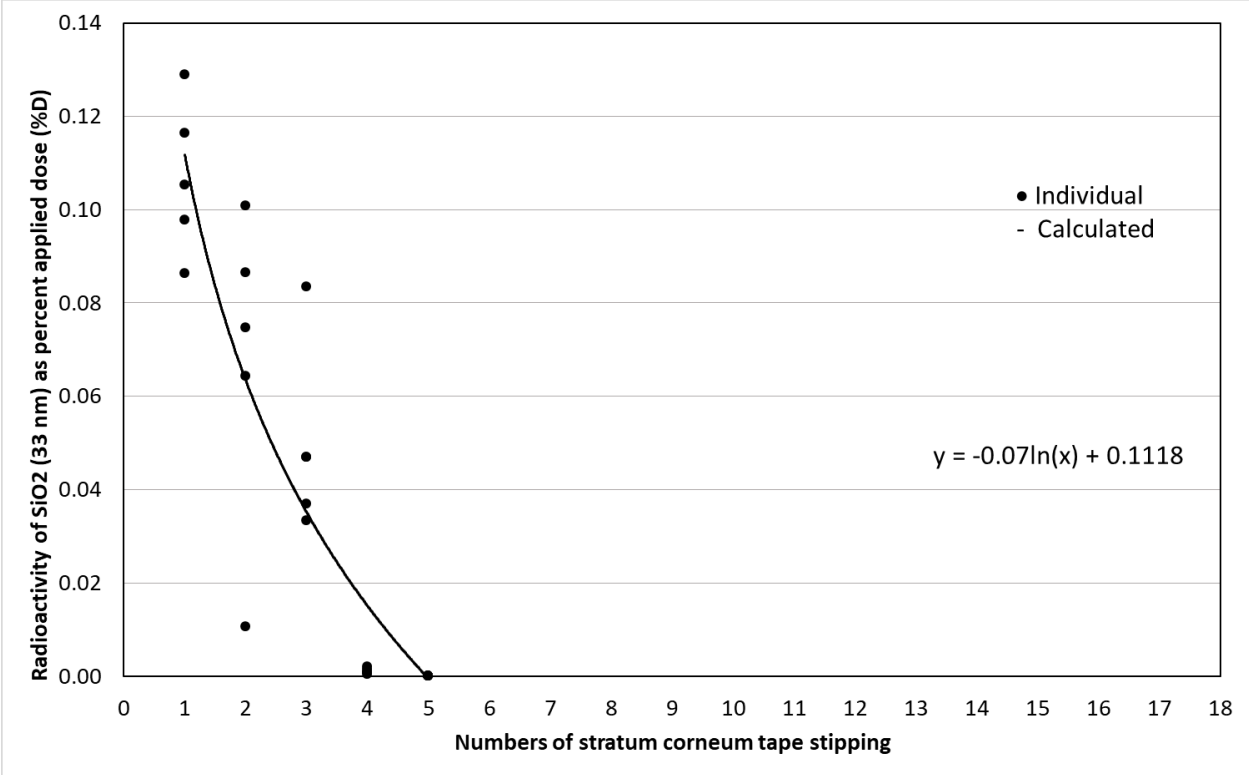


Figure 4. Dermatopharmacokinetic analysis of SiO<sub>2</sub> (78 nm) nanoparticles.